Phase-modulated photon antibunching in a two-level system coupled to two cavities

Changqing Wang,[1] Yu-Long Liu,[1] Rebing Wu,[2,3,*] and Yu-xi Liu[1,2,†]

[1]*Institute of Microelectronics, Tsinghua University, Beijing 100084, China*

[2]*Tsinghua National Laboratory for Information Science and Technology (TNList), Beijing 100084, China*

[3]*Department of Automation, Tsinghua University, Beijing 100084, China*

(Received 23 November 2016; published 11 July 2017)

Nonclassical light fields can be generated from two coupled cavities that are interacted with a two-level system. This scheme is drawing extensive attention because the mode coupling can reduce the requirement of coupling constants between the light fields and the two-level system. However, the effect of phase differences between different coupling constants on photon antibunching is always neglected. Considering a two-level system interacting with two coupled cavities, we analyze the statistical properties of the cavity field and show that the photon antibunching can be affected by the phase differences of coupling constants between the two-level system and the cavity modes, or between the cavity modes and the driving fields, and thus we can engineer the phases to optimally modulate single-photon sources or nonclassical light fields.

DOI: 10.1103/PhysRevA.96.013818

I. INTRODUCTION

Single-photon sources are indispensable ingredients in secure quantum communication and quantum information processing [1,2]. They are extensively applied to quantum key distribution [3,4], linear optical quantum computing [5–7], single-photon quantum memory [8–11], quantum metrology [12–15], quantum simulations [16,17], and interaction-free measurement [18]. Single-photon sources are usually obtained via spontaneous parametric down conversion or photon emission from a quantum emitter, e.g., an atomic or atomlike system [2]. In the latter case, photon blockade effect is highly noteworthy, in which single photons separated in time are emitted. The photon blockade can be measured via the photon intensity autocorrelation through the normalized equal-time second-order correlation function [19,20].

Photon blockade was first proposed in a Kerr-type nonlinear cavity, in which the photon-photon interaction is induced by a four-level atomic ensemble [21,22]. It is now well known that photon blockade can also be demonstrated in a cavity that is coupled to a two-level system, e.g., a cavity coupled to a trapped atom [23], a bimodal nanocavity coupled to a quantum dot [24], a bimodal microtoroidal resonator coupled to a two-level system [25], a photonic crystal resonator coupled to a quantum dot [26,27], a transmission line resonator coupled to a superconducting qubit [28,29], or a nitrogen vacancy center [30]. Several new platforms, including imbedding quantum dots in GaAs photonic crystals [31] and integrating colloidal quantum dots with SiN microdisks [32], have also been realized in experiments for engineering tunable and robust single-photon sources. In all of these studies, the two-level system and the cavity field are in the strong coupling regime to realize photon blockade. Furthermore, it has recently been shown that a two-level system coupled to a bimodal cavity with the mode coupling can exhibit the photon blockade effect even in the weak-coupling regime between the two-level system and the cavity fields [33].

However, we find that the photon antibunching in most of above studies [23–30,33] is obtained by tuning the amplitudes of different coupling constants in the systems, while the phase effect of the coupling constants on photon statistics has been ignored. It is well known that global phases of quantum superposed states can be ignored in quantum mechanics because they have no observable effects [34]. However, phase differences of amplitudes in superposed coefficients of quantum superpositions result in physically observable differences in measurement statistics, and thus the phase differences play a very important role in quantum mechanics. The phase effect of the coupling constant, between a cavity mode and a two-level system, was actually mentioned in demonstration of strong photon-atom coupling [35]. The coherent interaction between an atom and the evanescent fields of cavity modes in toroid resonators is influenced by the different locations of the atom around the circumference of the toroid. They found [35] that the spectrum of the forward flux is closely related to the atom's position which leads to phase difference of coupling constants between different modes and the atom.

Motivated by the photon blockade in coupled systems and the importance of the phases, here we theoretically study phase effects of coupling constants on photon blockade. We focus on the model that two cavities are coupled to a two-level system. The paper is organized as follows. In Sec. II, the theoretical model and the Hamiltonian are introduced. Section III presents detailed calculation of second-order correlation function for different parameters and shows how the phases can modulate photon statistics. In Sec. IV, phase effects in different situations are discussed via numerical analysis. Finally, we summarize our results and discuss experimental feasibility in Sec. V.

II. THEORETICAL MODEL

As schematically shown in Fig. 1, we study a system that a two-level system is coupled to two coupled cavities through modes A and B of cavity fields. We assume that the modes A and B locate in different cavities. The two-level system can be formed by either an atom, a quantum dot, a superconducting quantum circuit, or other two-level systems. For the generality

*rbwu@tsinghua.edu.cn

†yuxiliu@mail.tsinghua.edu.cn

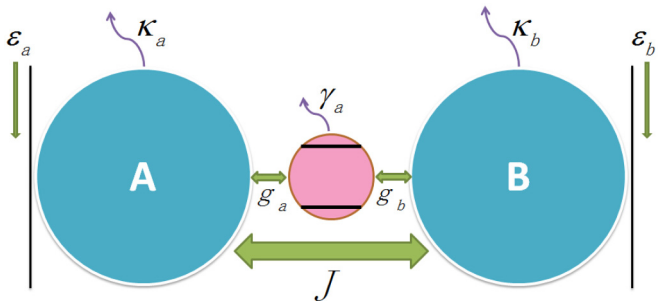

FIG. 1. Schematic diagram of a two-level system which is coupled to two cavities through modes A and B of cavity fields, respectively. Here we assume that the two modes reside in different cavities. The coupling between two modes via evanescent fields is described by the coupling constant J. The coupling constants between the two-level system and two modes are $g_a = |g_a|e^{i\theta_1}$ and $g_b = |g_b|e^{i\theta_2}$, respectively. Two modes of cavity fields are also separately driven by classical fields with the coupling constants $\varepsilon_a = |\varepsilon_a|e^{i\theta_a}$ and $\varepsilon_b = |\varepsilon_b|e^{i\theta_b}$. κ_a and κ_b represent the decay rates of the mode A and mode B, respectively. γ_a denotes the decay rate of the two-level system.

of discussions, we first do not specify it. We assume that two cavities have the same frequency ω and are driven by two classical fields, respectively. Thus the driven system can be described by the following Hamiltonian:

$$\begin{aligned} H &= \hbar\omega(a^\dagger a + b^\dagger b) + \hbar\omega_a\sigma_+\sigma_- + \hbar J(a^\dagger b + b^\dagger a) \\ &\quad + \hbar[g_a a^\dagger\sigma_- + g_b b^\dagger\sigma_- + \varepsilon_a a^\dagger e^{-i\omega_1 t} + \varepsilon_b b^\dagger e^{-i\omega_2 t} \\ &\quad + \text{H.c.}], \end{aligned} \tag{1}$$

where a and b ($a^\dagger$ and $b^\dagger$) are the annihilation (creation) operators of two modes of the cavities.

For the convenience of following presentation, we say that the operators a and b correspond to the mode A and mode B of two cavities, respectively. σ_- and σ_+ are ladder operators of the two-level system with the frequency ω_a. The parameter J denotes the coupling constant between two cavity modes, whereas the parameters g_a and g_b are the coupling constants between the two modes and the two-level system. We assume that the mode A is driven by a weak classical field with the frequency ω_1 and the coupling constant ε_a, and the mode B is driven by another weak classical field with the frequency ω_2 and the coupling constant ε_b. Here, the parameters g_a, g_b, ε_a, and ε_b are complex numbers, e.g., in experiments [35]. Moreover, the phases of the coupling constants ε_a and ε_b can be controlled by classical driving fields.

We now transform the Hamiltonian in Eq. (1) to the rotating reference frame at the frequency ω_1 of the driving field; then we have an effective Hamiltonian

$$\begin{aligned} H_{\text{eff}} &= \hbar\Delta(a^\dagger a + b^\dagger b) + \hbar\Delta_a\sigma_+\sigma_- + \hbar J(a^\dagger b + b^\dagger a) \\ &\quad + \hbar[(g_a a^\dagger + g_b b^\dagger)\sigma_- + \varepsilon_a a^\dagger + \varepsilon_b b^\dagger e^{-i\delta t} + \text{H.c.}], \end{aligned} \tag{2}$$

where $\Delta = \omega - \omega_1$ and $\Delta_a = \omega_a - \omega_1$ represent the detunings from the frequency ω_1 of the driving field to the frequency ω of cavity modes, and the frequency ω_a of the two-level system. The parameter $\delta = \omega_2 - \omega_1$ denotes the detuning from the frequency ω_1 of one driving field to the frequency ω_2 of another driving field.

The open system dynamics of the driven system can be described by a master equation. By taking into account the decay rates κ_i ($i = 1,2$) of cavity modes and γ_a of the two-level system, the master equation can be given as [27]

$$\frac{d\rho}{dt} = \frac{1}{i\hbar}[H_{\text{eff}}, \rho] + L\rho, \tag{3}$$

under Markov approximation with

$$L\rho = \frac{\kappa_1}{2}L(a)\rho + \frac{\kappa_2}{2}L(b)\rho + \frac{\gamma_a}{2}L(\sigma)\rho, \tag{4}$$

where $L(x)\rho = 2x\rho x^\dagger - x^\dagger x\rho - \rho x^\dagger x$. Below, we are only interested in the phase effect of the coupling constants on the statistical properties of the photons. Thus, for simplicity and without loss of generality, we assume $\omega_2 = \omega_1$ and $\omega_a = \omega$, i.e., $\delta = 0$ and $\Delta = \Delta_a$. We also assume $\kappa_1 = \kappa_2$, and that the dephasings of the two-level system and two cavity modes are negligibly small. Then, a convenient method of solving Eq. (3) is to use an effective non-Hermitian Hamiltonian

$$\begin{aligned} \widetilde{H} &= \hbar\Big(\Delta - i\frac{\kappa}{2}\Big)(a^\dagger a + b^\dagger b) \\ &\quad + \hbar\Big(\Delta - i\frac{\gamma_a}{2}\Big)\sigma_+\sigma_- + \hbar J(a^\dagger b + b^\dagger a) \\ &\quad + \hbar[(g_a a^\dagger + g_b b^\dagger)\sigma_- + \varepsilon_a a^\dagger + \varepsilon_b b^\dagger + \text{H.c.}], \end{aligned} \tag{5}$$

in the zero-temperature approximation [33]. Detailed deviation of the Hamiltonian in Eq. (5) can be found in Appendix A.

III. SECOND-ORDER CORRELATION FUNCTIONS

A. General solution

Equation (5) shows that physical properties of the modes A and B are equivalent, thus using the mode A as an example, we first analytically study the phase effect on photon statistical properties via the normalized equal-time second-order correlation function

$$g_{\text{A}}^{(2)}(0) = \frac{\langle a^\dagger a^\dagger a a\rangle}{\langle a^\dagger a\rangle^2} = \frac{\text{Tr}\,(\rho_{\text{ss}} a^\dagger a^\dagger a a)}{[\text{Tr}\,(\rho_{\text{ss}} a^\dagger a)]^2}, \tag{6}$$

where ρ_{ss} is the reduced density matrix of the system in the steady state.

Under the assumption that the two driving fields are very weak, the total excitation number of photons will not exceed two. In this case, the state of system can be approximately expressed as

$$\begin{aligned} |\varphi\rangle &= C_{0,0,-}|0,0,-\rangle + C_{1,0,-}|1,0,-\rangle + C_{0,1,-}|0,1,-\rangle \\ &\quad + C_{0,0,+}|0,0,+\rangle + C_{2,0,-}|2,0,-\rangle + C_{0,2,-}|0,2,-\rangle \\ &\quad + C_{1,1,-}|1,1,-\rangle + C_{1,0,+}|1,0,+\rangle + C_{0,1,+}|0,1,+\rangle, \end{aligned} \tag{7}$$

where $C_{i,j,\pm} = C_{i,j,\pm}(t)$ denote the coefficients [33] of the state $|\varphi\rangle$. In the weak-driving limit, we have the relation

$$\begin{aligned} |C_{0,0,-}| &\gg |C_{1,0,-}|, |C_{0,1,-}|, |C_{0,0,+}| \\ &\gg |C_{2,0,-}|, |C_{0,2,-}|, |C_{1,1,-}|, |C_{1,0,+}|, |C_{0,1,+}|. \end{aligned} \tag{8}$$

Using Eq. (6) and Eq. (7), the second-order correlation function $g_{\text{A}}^{(2)}(0)$ is given as

$$g_{\text{A}}^{(2)}(0) = \frac{2|C_{2,0,-}|^2}{|C_{1,0,-}|^4}, \tag{9}$$

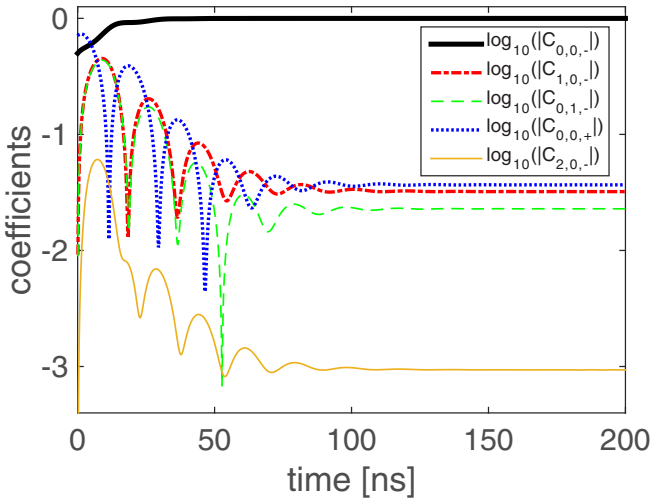

FIG. 2. Time evolution of the coefficients of the state by solving the dynamic Schrödinger equation. The initial state of the system is given by taking $C_{0,0,-}(0) = 0.5$, $C_{0,0,+}(0) = 1/\sqrt{2}$, $C_{1,1,-}(0) = 0.5$, and $C_{1,0,-}(0) = C_{0,1,-}(0) = C_{2,0,-}(0) = C_{0,2,-}(0) = C_{1,0,+}(0) = C_{0,1,+}(0) = 0$. The parameters are $g_a/2\pi = 20$ MHz, $g_b = g_a \exp(i2\pi/5)$, $\kappa/2\pi = 40$ MHz, $\gamma_a/2\pi = 1$ MHz, $\Delta/\kappa = 0.63$ MHz, $J = 30\kappa$, $\varepsilon_a = \gamma_a$, and $\varepsilon_b = \varepsilon_a \exp(i1.16\pi)$.

in the limit of the weak driving fields. The coefficients $C_{1,0,-}$ and $C_{2,0,-}$ can be solved from the Schrödinger equation

$$i\hbar\frac{\partial|\varphi\rangle}{\partial t} = \widetilde{H}|\varphi\rangle, \tag{10}$$

with the effective Hamiltonian $\widetilde{H}$ given in Eq. (5).

The numerical simulation of the time evolution for some coefficients is shown in Fig. 2 for a given initial state with the parameters of the system given. These coefficients evolve into stable values within the time scale of several hundreds of nanoseconds, with $C_{0,0,-}$ very close to 1. Other coefficients not shown in Fig. 2 also possess this steady-state feature and have the order of magnitude similar to $C_{2,0,-}$. Therefore, under the limit of the weak driving field and in the steady state, we can take $C_{0,0,-} \to 1$ as in Ref. [33], and solve the coefficients $C_{1,0,-}$ and $C_{2,0,-}$ from the following stationary Schrödinger equation:

$$\widetilde{H}|\varphi\rangle = 0. \tag{11}$$

Taking into account Eq. (5), Eq. (7), and Eq. (11), we derive a set of linear equations on coefficients of single excitation

$$\varepsilon_a^* C_{1,0,-} + \varepsilon_b^* C_{0,1,-} = 0, \tag{12}$$

$$\Delta_p C_{1,0,-} + J C_{0,1,-} + g_a C_{0,0,+} + \varepsilon_a = 0, \tag{13}$$

$$\Delta_p C_{0,1,-} + J C_{1,0,-} + g_b C_{0,0,+} + \varepsilon_b = 0, \tag{14}$$

$$\Delta_d C_{0,0,+} + g_a^* C_{1,0,-} + g_b^* C_{0,1,-} = 0, \tag{15}$$

where the detunings are

$$\Delta_p = \Delta - i\frac{\kappa}{2}, \tag{16}$$

$$\Delta_d = \Delta - i\frac{\gamma_a}{2}. \tag{17}$$

Because Eq. (12) always holds in the limit of the weak driving, we can solve Eqs. (13)–(15) to obtain the coefficients $C_{1,0,-}$, $C_{0,1,-}$, and $C_{0,0,+}$ as

$$C_{1,0,-} = \frac{\varepsilon_a(\Delta_p\Delta_d - |g_b|^2) + \varepsilon_b(g_a g_b^* - J\Delta_d)}{X}, \tag{18}$$

$$C_{0,1,-} = \frac{\varepsilon_a(g_a^* g_b - J\Delta_d) + \varepsilon_b(\Delta_p\Delta_d - |g_a|^2)}{X}, \tag{19}$$

$$C_{0,0,+} = \frac{\varepsilon_a(J g_b^* - \Delta_p g_a^*) + \varepsilon_b(J g_a^* - \Delta_p g_b^*)}{X}. \tag{20}$$

The parameter X is expressed as

$$X = \left(J^2 - \Delta_p^2\right)\Delta_d + \Delta_p(|g_a|^2 + |g_b|^2) - J[g_a^* g_b + \text{H.c.}]. \tag{21}$$

We can also obtain the equations of coefficients for two excitation as

$$\sqrt{2}\Delta_p C_{2,0,-} + J C_{1,1,-} + g_a C_{1,0,+} + \varepsilon_a C_{1,0,-} = 0, \tag{22}$$

$$\sqrt{2}\Delta_p C_{0,2,-} + J C_{1,1,-} + g_b C_{0,1,+} + \varepsilon_b C_{0,1,-} = 0, \tag{23}$$

$$2\Delta_p C_{1,1,-} + \sqrt{2}J(C_{0,2,-} + C_{2,0,-}) + g_a C_{0,1,+} + g_b C_{1,0,+} + \varepsilon_a C_{0,1,-} + \varepsilon_b C_{1,0,-} = 0, \tag{24}$$

$$(\Delta_p + \Delta_d)C_{1,0,+} + J C_{0,1,+} + \sqrt{2}g_a^* C_{2,0,-} + g_b^* C_{1,1,-} + \varepsilon_a C_{0,0,+} = 0, \tag{25}$$

$$(\Delta_p + \Delta_d)C_{0,1,+} + J C_{1,0,+} + g_a^* C_{1,1,-} + \sqrt{2}g_b^* C_{0,2,-} + \varepsilon_b C_{0,0,+} = 0. \tag{26}$$

It is straightforward to obtain a complete solution for coefficients of two excitation, and accordingly the second-order correlation function. But it is not easy to see physics from a complicated formula. From the above derivations, we can find that $g_{\rm A}^{(2)}(0)$ is related to both the amplitudes and phases of $g_a, g_b, \varepsilon_a, \varepsilon_b$, and also the coupling constant J between two modes of the cavities when all of these parameters are not zero. Below, we further discuss phase effects on the photon antibunching for some special cases of the parameters.

B. Second-order correlation function for $J \neq 0$

From the above discussions, we know that the second-order correlation function can be modulated by the amplitudes and phases of $g_a, g_b, \varepsilon_a, \varepsilon_b$ when the coupling constant $J \neq 0$. We now further discuss some special cases for $J \neq 0$ when the mode A is coupled to the two-level system and also driven by a classical field.

For the case $J \neq 0$ and $\varepsilon_b = 0$, that is, there is coupling between modes of the cavities, but the mode B is not driven. In this case, the solution of the second-order correlation function is still very complex. The following numerical simulation will show that $g_{\rm A}^{(2)}(0)$ is independent of ε_a, but is related to both the amplitudes and phases of the coupling constants g_a and g_b.

For the case $J \neq 0$ and $g_b = 0$, that is, the mode B is not coupled to the two-level system but is driven, the following

numerical simulation shows that $g_{\mathrm{A}}^{(2)}(0)$ is independent of both ε_a and ε_b, and is only related to the amplitude of g_a.

Therefore, it is clear that the coupling constant g_b (g_a) between the two-level system and the mode B (mode A) plays a crucial role for the phase effect on the statistical properties of the photons when $J \neq 0$ and only one driving field is applied. The physical meaning of this result can be explained by the interference picture as in Ref. [33]. When $g_b = 0$, the interaction between mode A and the two-level system is achieved only through their direct coupling described by g_a. When both J and g_b are nonzero, there comes an alternative, indirect way to realize this kind of interaction: mode A is coupled to mode B through J, and mode B is coupled to the two-level system through g_b. This results in a new transition path between $|1,0,-\rangle$ and $|2,0,-\rangle$, which involves the effect of phase difference. For example, the phase difference between g_a and g_b has influence on the quantum interference between the two transition paths (1) $|1,0,-\rangle \xrightarrow{\varepsilon_a} |2,0,-\rangle$ and (2) $|1,0,-\rangle \xrightarrow{g_a^*} |0,0,+\rangle \xrightarrow{\varepsilon_a} |1,0,+\rangle \xrightarrow{g_b} |1,1,-\rangle \xrightarrow{J} |2,0,-\rangle$. Therefore, the photon antibunching is modulated by the phase difference between g_a and g_b in this case.

C. Second-order correlation function for $J = 0$

To better understand the phase effects on photon statistics, we consider the simpler case that $J = 0$, i.e., in absence of the mode-mode coupling. Under this circumstance, Eqs. (12)–(26) can be greatly reduced, which, combined with Eq. (9), lead to (see Appendix B for derivation)

$$g_{\mathrm{A}}^{(2)}(0) = \left|\frac{1+R_p}{1+R_c}\right|^2, \tag{27}$$

with

$$R_p = \frac{\Delta_p^2\left(\Delta_d\Delta_p - |g_b|^2 + |g_a|^2 + 2\varepsilon_a^{-1}\varepsilon_b g_a g_b^*\right)}{\left(\Delta_d\Delta_p - |g_b|^2 + \varepsilon_a^{-1}\varepsilon_b g_a g_b^*\right)^2}, \tag{28}$$

$$R_c = \frac{\Delta_p^2}{\Delta_d\Delta_p - |g_b|^2 - |g_a|^2}. \tag{29}$$

Denote $g_a = |g_a|e^{i\theta_1}$, $g_b = |g_b|e^{i\theta_2}$, $\varepsilon_a = |\varepsilon_a|e^{i\theta_a}$, and $\varepsilon_b = |\varepsilon_b|e^{i\theta_b}$. This result shows that, in general, $g_{\mathrm{A}}^{(2)}(0)$ can be modulated by the phases if and only if all coupling constants ε_a, ε_b, g_a, and g_b are nonzero, and it is dependent only on the phase of the term $\varepsilon_a^{-1}\varepsilon_b g_a g_b^*$, i.e.,

$$\Theta = (\theta_b - \theta_a) - (\theta_2 - \theta_1), \tag{30}$$

which can be changed by tuning any of the four phase variables. Moreover, the dependence of $g_{\mathrm{A}}^{(2)}(0)$ on $\varepsilon_a^{-1}\varepsilon_b g_a g_b^*$ also indicates that, in the weak-coupling limit, only the relative strength $|\varepsilon_b|/|\varepsilon_a|$ of the driving field, but not their absolute amplitudes, affects the photon antibunching.

This result can also be understood by the interference picture. Considering the two transition paths (1) $|1,0,-\rangle \xrightarrow{\varepsilon_a} |2,0,-\rangle$ and (2) $|1,0,-\rangle \xrightarrow{\varepsilon_b} |1,1,-\rangle \xrightarrow{g_b^*} |1,0,+\rangle \xrightarrow{g_a} |2,0,-\rangle$, we see that the quantum interference is influenced by the phase difference between g_a, g_b, ε_a, and ε_b. It can also be inferred that if g_b or ε_b is zero, then the second path is cut off. The excitation from $|1,0,-\rangle$ to $|2,0,-\rangle$ can only be realized by ε_a, and thus the phase effect disappears. This inference is confirmed by the following discussion.

TABLE I. Comparison of different parameters for photon antibunching in a system of a two-level system coupled to two cavities. In each case, J, g_b, and ε_b are marked by "√" if nonzero. For each parameter ε_a, ε_b, g_a, and g_b, the second-order correlation function can be related to both the amplitude and phase (marked by Yes), only the amplitude [marked by Yes (Amp.)], or neither the amplitude nor the phase (marked by No).

Cases	J	g_b	ε_b	ε_a	ε_b	g_a	g_b
G	√	√	√	Yes	Yes	Yes	Yes
B.1	√	√		No	No	Yes	Yes
B.2	√		√	No	No	Yes (Amp.)	No
B.3	√			No	No	Yes (Amp.)	No
C.1		√	√	Yes	Yes	Yes	Yes
C.2		√		Yes (Amp.)	No	Yes (Amp.)	Yes (Amp.)
C.3			√	No	No	Yes (Amp.)	No
C.4				No	No	Yes (Amp.)	No

For the case that both $J = 0$ and $g_b = 0$, the mode B becomes free and the system is reduced to a two-level system coupled to a cavity mode driven by a classical field [26]. In this case, $g_{\mathrm{A}}^{(2)}(0)$ is independent of ε_a and the phase of g_a. The statistical properties of photons are affected only by the amplitude of g_a. The case that $J = 0$, $g_b = 0$, and $\varepsilon_b = 0$ is a more special one for the case that $J = 0$ and $g_b = 0$; thus, in this case, the phase has no effect on the statistics of photons. For the case $J = 0$ and $\varepsilon_b = 0$, we find that $g_{\mathrm{A}}^{(2)}(0)$ is related to ε_a, g_a, and g_b, but only their amplitudes rather than their phases.

The effects of the parameters on the statistical properties of photons for different cases are summarized in Table I. When the mode A is coupled to the two-level system and is driven by the classical field, we find that the phases of the parameters ε_a, ε_b, g_a, and g_b affect the statistical properties of photons in mode A in the following cases: (i) both $g_b \neq 0$ and $\varepsilon_b \neq 0$ for $J \neq 0$, i.e., the case G in Table I; (ii) $g_b \neq 0$ but $\varepsilon_b = 0$ for $J \neq 0$, i.e., the case B.1 in Table I; (iii) both $g_b \neq 0$ and $\varepsilon_b \neq 0$ for $J = 0$, i.e., the case C.1 in Table I.

IV. NUMERICAL SIMULATIONS

To further show how the values of the phase parameters affect the photon antibunching, in this section, we numerically solve the Schrödinger equation in the steady state and study the photon antibunching, discussed above analytically. Because we are interested in the phase effect, thus we only focus on the cases G, B.1, and C.1 in Table I.

A. Case with mode coupling ($J \neq 0$) and $\varepsilon_b = 0$

We first study the case B.1 in Table I, that is, two cavity modes are coupled to each other and also coupled to a two-level system, but the mode B is not driven, i.e., $\varepsilon_b = 0$. The mode A is driven by a classical field with the coupling constant ε_a. As shown in Table I, the statistical property of the mode A is irrelevant to the phase of its driving field, but controlled by the phase difference of the coupling constants g_a and g_b. We

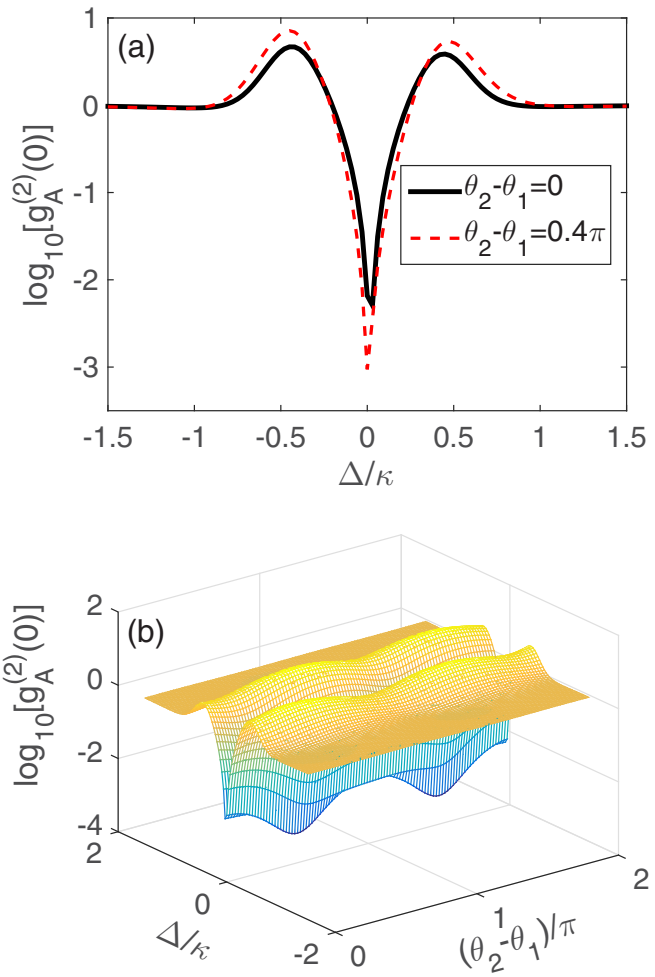

FIG. 3. (a) Second-order correlation function $g_A^{(2)}(0)$ of the mode A is plotted as a function of Δ/κ for the case B.1 in Table I with and without the phase difference between g_b and g_a. The black-solid (red-dashed) curve represents $g_A^{(2)}(0)$ in logarithmic scale with $\theta_2 - \theta_1 = 0$ ($\theta_2 - \theta_1 = 0.4\pi$). (b) The second-order correlation function $g_A^{(2)}(0)$ of the mode A is plotted as a function of Δ/κ and $\theta_2 - \theta_1$ for the case B.1 in Table I. Other parameters are given as $|g_b|/2\pi = |g_a|/2\pi =$ 20 MHz, $\kappa/2\pi = 40$ MHz, $\gamma_a/2\pi = 1$ MHz, $J = 30\kappa$, $|\varepsilon_a| = \gamma_a$, $\theta_a = 0$, and $\varepsilon_b = 0$.

assume $g_a = |g_a|e^{i\theta_1}$ and $g_b = |g_b|e^{i\theta_2}$. The effect of the phase difference $\theta_2 - \theta_1$ on the photon antibunching is shown in Fig. 3(a), where the second-order correlation function $g_A^{(2)}(0)$ is plotted as a function of Δ/κ with or without the phase difference for other given parameters. By optimizing the phase difference, we find that the minimum value of the second-order correlation function at $\Delta = 0$ can be lower than the minimum value of 6.0×10^{-3} given in Ref. [33] when $\theta_2 - \theta_1 = 0$. This means that the photon antibunching can be optimized by changing the phase difference between g_b and g_a.

To clearly see the effects of the phase difference between g_b and g_a, the second-order correlation function $g_A^{(2)}(0)$ versus Δ/κ and the phase difference $\theta_2 - \theta_1$ is calculated and shown in Fig. 3(b). The range of variation of $g_A^{(2)}(0)$ is more than one order of magnitude when the phase difference $\theta_2 - \theta_1$ is changed, and the minimum $g_A^{(2)}(0)$ can reach 6.0×10^{-4} when $\theta_2 - \theta_1 = 1.5\pi$, compared to 6.0×10^{-3} when $\theta_2 - \theta_1 = 0$ shown in Ref. [33]. That is, Fig. 3 clearly shows that the photon antibunching of the mode A can be modulated by the phase difference between g_b and g_a. Figure 3 also shows that the antibunching can be observed with weak-coupling strengths between the cavity modes and the two-level system, e.g., $|g_a|/\kappa = |g_b|/\kappa = 0.5$. As discussed in Sec. III, the effects of the phase difference on the antibunching can be explained from the interference picture as in Ref. [33]. That is, the interference patterns and the induced photon antibunching can be periodically modulated via the phase difference.

B. Case without mode coupling ($J = 0$)

We now discuss the phase effect on the photon antibunching for the case C.1 in Table I. In this case, the photon antibunching is affected by the phases only when two cavity modes are coupled to a two-level system and are driven by two classical fields, respectively. The second-order correlation function $g_A^{(2)}(0)$ is related to both amplitudes and phases of ε_a, ε_b, g_a, g_b. The phase will not have an effect on the antibunching when any one of the above four parameters is equal to zero.

When all the four parameters are nonzero, only the phase variable Θ defined by Eq. (30) takes effect. Without loss of generality, we tune the phase difference $\theta_b - \theta_a$ between two driving fields, and fix the value of $\theta_2 - \theta_1$ at 0.4π, i.e., $\Theta = \theta_b - \theta_a - 0.4\pi$. Figure 4 plots the second-order correlation function $g_A^{(2)}(0)$ versus Δ/κ under various values of $\theta_b - \theta_a$. We find that the second-order correlation function $g_A^{(2)}(0)$ is up to 10^6 when $\theta_b - \theta_a = 0.4\pi$, which indicates a photon bunching effect. However, by changing $\theta_b - \theta_a$, $g_A^{(2)}(0)$ changes dramatically and becomes less than 1 ($\log_{10}[g_A^{(2)}(0)] < 0$) when $\theta_b - \theta_a$ gets close to 1.16π. Thus the photon bunching

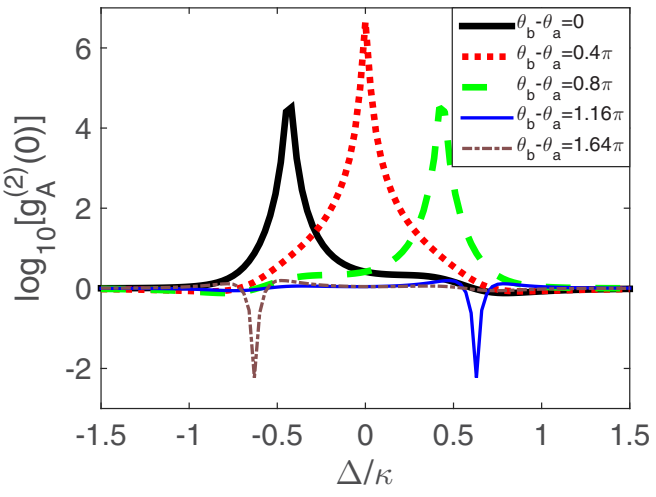

FIG. 4. Second-order correlation function $g_A^{(2)}(0)$ vs Δ/κ for the case C.1 listed in Table I. The colored curves represent $g_A^{(2)}(0)$ in logarithmic scale for $\theta_b - \theta_a = 0$, 0.4π, 0.8π, 1.16π, and 1.64π, respectively. There is no coupling between the modes A and B, i.e., $J = 0$. The cavity mode B is coupled to the two-level system with coupling constant $g_b = |g_b|e^{i\theta_2}$. Here, we assume $|g_b|/2\pi = 20$ MHz and $\theta_2 - \theta_1 = 0.4\pi$. Other parameters are the same as those in Fig. 3.

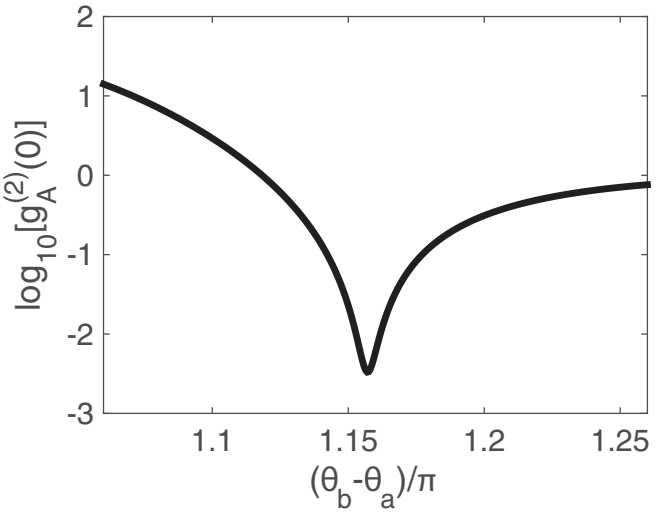

FIG. 5. Second-order correlation function $g_A^{(2)}(0)$ vs $\theta_b-\theta_a$ around 1.16π for the case C.1 listed in Table I. The curve represents $g_A^{(2)}(0)$ in logarithmic scale for $\Delta/\kappa=0.63$. Other parameters are the same as those in Fig. 4.

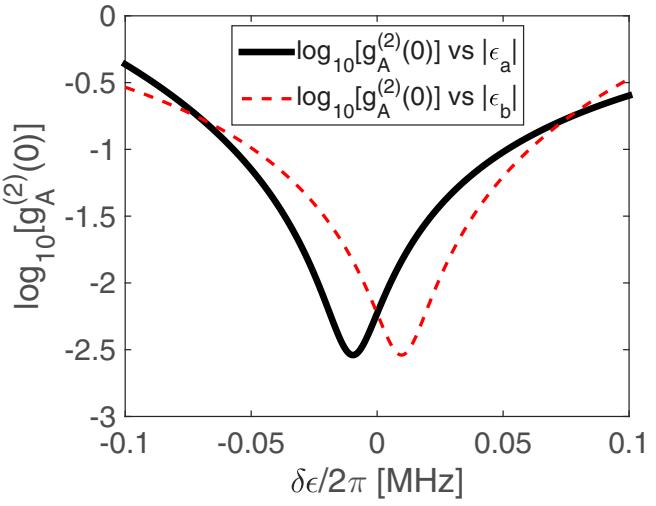

FIG. 6. Second-order correlation function $g_A^{(2)}(0)$ vs $|\varepsilon_a|$ and $|\varepsilon_b|$ around $\varepsilon_0/2\pi=1$ MHz for the case C.1 listed in Table I. The colored curves represent $g_A^{(2)}(0)$ in logarithmic scale for $\theta_b-\theta_a=1.16\pi$ and $\Delta/\kappa=0.63$. $\delta\varepsilon$ represents $|\varepsilon_a|-\varepsilon_0$ and $|\varepsilon_b|-\varepsilon_0$ for the two curves, respectively. Other parameters are the same as those in Fig. 4.

effect has been changed to the photon antibunching effect with the change of the phase difference of g_a and g_b. This shows the transition from photon bunching to photon antibunching of mode A. The calculation of minimal $g_A^{(2)}(0)$ over the range $\theta_b-\theta_a\in(0,2\pi)$ indicates that $g_A^{(2)}(0)$ can be lowered to 5.9×10^{-3}, when $\theta_b-\theta_a=1.16\pi$ and $\Delta/\kappa=0.63$, or $\theta_b-\theta_a=1.64\pi$ and $\Delta/\kappa=-0.63$. Therefore, photon antibunching can be achieved and enhanced by simply tuning the phase difference of ε_a and ε_b between the two driving fields applied to the cavity modes.

Furthermore, the photon bunching and antibunching are sensitive to phase changes around the optimal points. Figure 5 plots the second-order correlation function $g_A^{(2)}(0)$ around the optimal antibunching point $\theta_b-\theta_a=1.16\pi$ with $\Delta/\kappa=0.63$. It indicates that a phase change, e.g., 0.02π, could alter the magnitude of $g_A^{(2)}(0)$ by one order. Similarly, the bunching effect is also sensitive to the phase difference. Moreover, the amplitudes of driving fields are also crucial for the degree of photon antibunching. Figure 6 plots $g_A^{(2)}(0)$ with the fluctuation of field amplitudes $|\varepsilon_a|$ and $|\varepsilon_b|$, respectively, at the optimal antibunching point with $\theta_b-\theta_a=1.16\pi$ and $\Delta/\kappa=0.63$. The change of $|\varepsilon_a|/2\pi$ or $|\varepsilon_b|/2\pi$ by, e.g., 0.03 MHz would lead to a change of $g_A^{(2)}(0)$ by one order of magnitude.

Finally, it can be verified using similar numerical simulations that photon antibunching is not very sensitive to the amplitudes of coupling constants between the cavities and the two-level system. Therefore, the control of driving fields, both their amplitudes and phase difference, is important for achieving a robust photon antibunching in this case.

C. General case for all nonzero parameters

For the general case labeled as G in Table I in which all parameters are nonzero, $g_A^{(2)}(0)$ is related to both amplitudes and phases of all coupling constants ε_a, ε_b, g_a, and g_b. Below, the definitions of the phase differences $\theta_b-\theta_a$ and $\theta_2-\theta_1$ are the same as those in Sec. IV B. To further study the effects of these coupling parameters on the photon antibunching, the second-order correlation function $g_A^{(2)}(0)$ is shown in Fig. 7 and Fig. 8 for the case G in Table I. A significant difference between the case G and the case C.1 is that the photon antibunching effect becomes significant when the amplitude of the driving field of the mode B is much smaller than that of the mode A, e.g., $|\varepsilon_b|=0.1|\varepsilon_a|$. That is, the general case discussed here is more realistic than the case B.1, with the existence of the driving field of the mode B, which is much weaker than that of the mode A. Besides, the photon antibunching is very sensitive to the value of the mode coupling constant

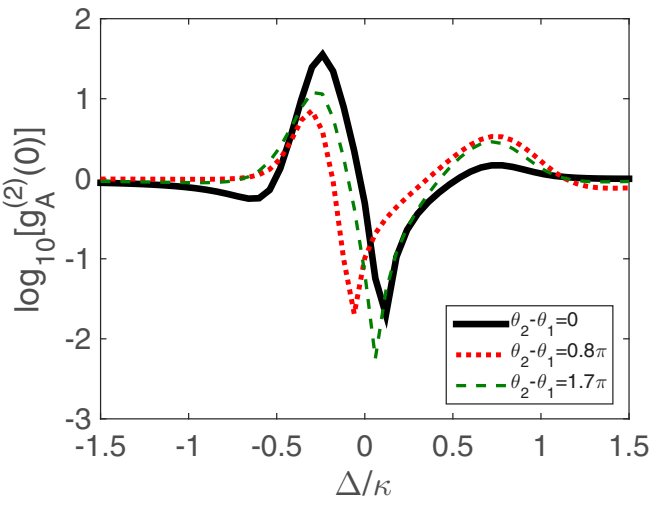

FIG. 7. Second-order correlation function $g_A^{(2)}(0)$ of the mode A vs Δ/κ in the case G listed in Table I. The colored curves represent $g_A^{(2)}(0)$ in logarithmic scale for $\theta_2-\theta_1=0$, 0.8π, and 1.7π, respectively. The coupling constant between the modes A and B is assumed as $J/\kappa=5$. Here, we assume $|\varepsilon_b|=|\varepsilon_a|/10$ and $\theta_b-\theta_a=0$. Other parameters are the same as those in Fig. 3.

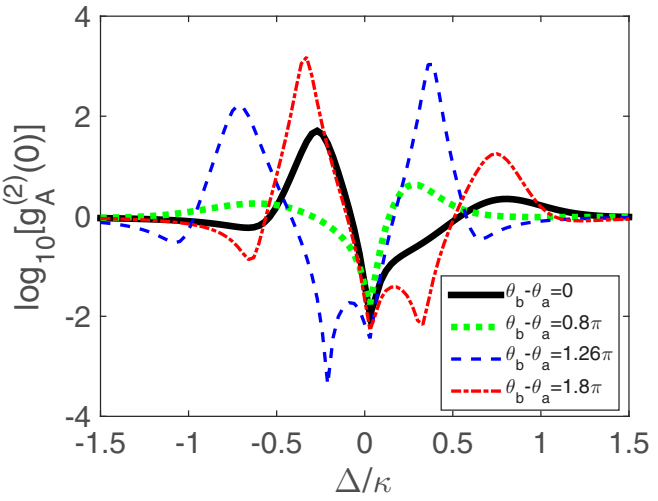

FIG. 8. Second-order correlation function $g_A^{(2)}(0)$ of the mode A vs Δ/κ in the case G listed in Table I. The colored curves represent $g_A^{(2)}(0)$ in logarithmic scale for $\theta_b - \theta_a = 0$, 0.8π, 1.26π, and 1.8π, respectively. The coupling constant between the modes A and B is assumed as $J/\kappa = 5$. The coupling constant of the mode B to the two-level system is assumed as $g_b = |g_b|e^{i\theta_2}$ with $|g_b|/2\pi = 20$ MHz. We also assume $|\varepsilon_b| = |\varepsilon_a|/10$ and $\theta_2 - \theta_1 = 0.4\pi$. Other parameters of the system are the same as those in Fig. 3.

J. As is shown in Fig. 7, the photon antibunching is very strong at $\Delta/\kappa = 0.06$, in which $g_A^{(2)}(0) = 5.7 \times 10^{-3}$ when $\theta_2 - \theta_1 = 1.7\pi$. In fact, this effect follows a pattern similar to the case B.1, except that the driving field of the mode B is added. This driving field distorts the symmetric distribution of the second-order correlation function about the resonant point $\Delta = 0$. Furthermore, the effect of $\theta_2 - \theta_1$ becomes less important compared to the case B.1. It thus provides another way to obtain a single-photon source. In this case, the photon antibunching is less sensitive to the phase shift of the coupling constants between the two-level system and cavities.

In Fig. 8, $g_A^{(2)}(0)$ is plotted as a function of Δ/κ with different values of $\theta_b - \theta_a$ for $\theta_2 - \theta_1 = 0.4\,\pi$. It shows that near $\Delta = 0$, the photon antibunching is always strong no matter what the phase difference $\theta_b - \theta_a$ is, with the second-order correlation function $g_A^{(2)}(0)$ being about 10^{-2}. That is, near $\Delta = 0$, the photon antibunching is insensitive to the phases of the driving fields. However, if the detuning goes far from the resonant point $\Delta = 0$, the second-order correlation function can be further reduced to reach 4.29×10^{-4} when $\theta_b - \theta_a = 1.26\pi$ and $\Delta/\kappa = -0.21$. Therefore, the phase difference of the driving fields can still be used to enhance the photon antibunching.

Thus, from Fig. 7 and Fig. 8, we know that (1) near the resonant point $\Delta = 0$, the second-order correlation function $g_A^{(2)}(0)$ is stable and not very sensitive to the phase shift of coupling constants and (2) if we tune both the phase difference $\theta_b - \theta_a$ of the driving fields and the detuning Δ, the photon antibunching in the mode A can be further optimized.

V. EXPERIMENTAL REALIZATION

Let us now discuss possible experimental realization. The coupled system between a semiconductor bimodal microcavity and a quantum dot [36–39] is a promising platform. When the clockwise (CW) mode is driven by a laser, the counterclockwise (CCW) mode is generated due to surface scattering of the microcavity. This corresponds to the case B in Sec. III. Inspired by the theoretical works in Refs. [35] and [40], the field distributions of the clockwise (CW) and counterclockwise (CCW) modes have an azimuthal spatial dependence. Thus the phases of coupling constants between the two-level system and the two modes can be tuned by varying the position of the two-level system relative to the azimuthal distribution of the modes when the sample is fabricated. Furthermore, if the two optical modes are both driven by lasers, the case C in Sec. III can be realized, when the scattering-induced mode coupling does not exist. In this case, both the phases and the amplitudes of ε_a and ε_b can be controlled by the driving fields in the optical fibers or waveguides coupled to the microcavity. Besides, great potential lies in new tunable and robust platforms, with cutting-edge technologies of coupling quantum dots to microdisks [41].

Another promising platform is the columnar semiconductor microcavity interacting with the semiconductor quantum dot [42–44]. The optical modes in the semiconductor microcavity are coupled to each other through a scatterer or other defects. Especially, the coupling between different polarized optical modes with the same eigenfrequencies is observed [45,46]. In addition, the quantum well embedded in the semiconductor microcavity also shows the potential for studying multibody interactions [47]. Here, the change of the relative phase between the input fields of these two optical modes is controlled by tuning the phases of the external pump lasers. Therefore, our proposal may be feasible in the columnar semiconductor microcavity systems.

Recently, photon blockade was realized with a quantum dot, strongly coupled to a photonic crystal nanocavity [48–52], where only one optical mode is used. In addition, a lossy bimodal optical cavity is fabricated for observing the unconventional photon blockade [24], and the photon blockade is also optimized versus the ratio of the coupling strengths between the quantum dot and the two cavity modes. Based on such controllable coupling strengths and the external pump fields, our proposal is hopefully applied to the realization of single-photon sources with the photonic crystal structure [53].

Besides the optical frequency domain, tunable single-photon source in the microwave domain is a key element in a series of prospective quantum technologies and applications. The photon blockade at microwave frequencies was observed by using correlation function measurements [54–57]. However, the photon blockade is still weak and only limited to the single cavity mode case. To enhance the photon blockade and its robustness to the dephasing of the superconducting artificial atoms, the interactions between different microwave cavity fields should be explored. The multimode cavity QED systems are proposed for photonic memories, efficient Purcell filters, and quantum simulations [58]. The mode coupling between different cavity fields has been studied and used for, e.g., separating photon storage and qubit readout [59], deterministically encoding quantum information [60], and studying the multimode correlations from vacuum fluctuations [61]. Based on such controllable mode coupling between the cavity

fields and tunable coupling strengths between the cavity fields and the superconducting artificial atom, our proposal is also feasible in superconducting quantum circuits [62–64].

In view of rapid progress of optomechanics, we finally mention that our study here is also possibly realized in the system of two cavity fields, coupled to a mechanical resonator via radiation pressure or the hybrid optomechanical polariton systems [65–69]. Corresponding to the bimodal optical fields, here a phase and amplitude tunable pump for the mechanical mode should be introduced. This can be realized by the related experiments [70–75] . Based on the experimental feasibility discussed above, we hope that our study will be helpful for generating stable and controllable single-photon sources in future experiments.

VI. CONCLUSION

Using one of the modes of two cavities as an example, we study the phase effect on the photon antibunching in a two-level system coupled to modes of two cavities with or without mode coupling. We mainly study how the phases of the coupling constants (g_a, g_b, ε_a, and ε_b) affect the second-order correlation function $g^{(2)}(0)$. We mention that the parameters g_a and g_b denote the coupling between the two-level system and cavity fields, while the parameters ε_a and ε_b denote the coupling between the cavity fields and the driving fields. We find that the phases of these coupling constants affect $g^{(2)}(0)$ in the following three cases.

(i) Two modes of two cavities are coupled to each other and the two-level system, and they are driven by classical fields. In this case, both the phase differences, between the coupling parameters g_a and g_b, and between the coupling parameters ε_a and ε_b, affect the photon antibunching. Our numerical calculation shows that the minimum value of $g^{(2)}(0)$ can reach about the order of 10^{-4} by optimizing the parameters. We also find that near the resonant point ($\Delta = 0$), the photon antibunching is not sensitive to phase differences.

(ii) Two modes of two cavities are coupled to each other and also coupled to the two-level system, while one of the modes is driven by a classical field. In this case, only the phase difference between the coupling parameters g_a and g_b affect the photon antibunching, whereas the phase of the driving field has no effect. The minimum value of $g^{(2)}(0)$ can also reach the order of 10^{-4} by optimizing the parameters.

(iii) Two modes of two cavities are coupled to the two-level system and driven by classical fields, but there is no mode coupling between them. In this case, both the phase differences, between the coupling parameters g_a and g_b and between the coupling parameters ε_a and ε_b, affect the photon antibunching. The minimum value of $g^{(2)}(0)$ can also reach the order of 10^{-3} by optimizing the parameters, and the transition between photon bunching and antibunching is achieved by tuning the phase differences and the detuning. Moreover, the optimal antibunching point can be reached by the control of amplitudes and phases of the driving fields, and this point is insensitive to the change of coupling parameters g_a and g_b.

Based on the studies above, we conclude that the cases (i) and (iii) have a larger chance to be experimentally implemented, because the phase difference of the driving fields is much easier to adjust than that of the coupling constants between the two-level system and the cavity modes. In the case (ii), the phase of the driving field does not affect the antibunching. Comparing the case (i) with the case (iii), we know that the photon antibunching becomes better when the mode coupling is introduced.

In summary, we find that the phases of the coupling constants can be used to adjust the photon antibunching of cavity fields in a two-level system coupled to two modes of two cavities. Although we only study the statistical properties for one of modes, the other one also has the same behavior because these two modes of two cavities are equivalent to each other. For the case that there is one driving field, the statistical properties can be very different if the two-level system is placed into different places of the cavities. Furthermore, if two classical fields are applied to the modes, then the statistical properties are much easier to adjust via these two external fields.

ACKNOWLEDGMENTS

Y.X.L. is supported by the National Basic Research Program of China (973 Program) under Grant No. 2014CB921401, the Tsinghua University Initiative Scientific Research Program, and the Tsinghua National Laboratory for Information Science and Technology (TNList) Cross-discipline Foundation.

APPENDIX A: DERIVATION OF THE EFFECTIVE NON-HERMITIAN HAMILTONIAN

Using the effective Hamiltonian of the system in Eq. (2), the master equation in Eq. (3) can be calculated as

$$\begin{aligned}\frac{d\rho}{dt} &= -i[\Delta(a^\dagger a + b^\dagger b) + \Delta_a\sigma_+\sigma_- + J(a^\dagger b + b^\dagger a)\\ &\quad + \{(g_a a^\dagger + g_b b^\dagger)\sigma_- + \varepsilon_a a^\dagger + \varepsilon_b b^\dagger e^{-i\delta t} + \text{H.c.}\},\rho]\\ &\quad + \frac{\kappa_1}{2}(2a\rho a^\dagger - a^\dagger a\rho - \rho a^\dagger a)\\ &\quad + \frac{\kappa_2}{2}(2b\rho b^\dagger - b^\dagger b\rho - \rho b^\dagger b)\\ &\quad + \frac{\gamma_a}{2}(2\sigma_-\rho\sigma_+ - \sigma_+\sigma_-\rho - \rho\sigma_+\sigma_-). \qquad \text{(A1)}\end{aligned}$$

We make an approximation that the terms $2a\rho a^\dagger$, $2b\rho b^\dagger$, and $2\sigma_-\rho\sigma_+$ are neglected. Thus the master equation in Eq. (A1) can be rewritten as

$$\begin{aligned}\frac{d\rho}{dt} &\approx -i[\Delta(a^\dagger a + b^\dagger b) + \Delta_a\sigma_+\sigma_- + J(a^\dagger b + b^\dagger a)\\ &\quad + \{(g_a a^\dagger + g_b b^\dagger)\sigma_- + \varepsilon_a a^\dagger + \varepsilon_b b^\dagger e^{-i\delta t} + \text{H.c.}\},\rho]\\ &\quad - \frac{\kappa_1}{2}(a^\dagger a\rho + \rho a^\dagger a) - \frac{\kappa_2}{2}(b^\dagger b\rho + \rho b^\dagger b)\\ &\quad - \frac{\gamma_a}{2}(\sigma_+\sigma_-\rho + \rho\sigma_+\sigma_-)\\ &= -i[\Delta(a^\dagger a + b^\dagger b) + \Delta_a\sigma_+\sigma_- + J(a^\dagger b + b^\dagger a)\\ &\quad + \{(g_a a^\dagger + g_b b^\dagger)\sigma_- + \varepsilon_a a^\dagger + \varepsilon_b b^\dagger e^{-i\delta t} + \text{H.c.}\},\rho]\\ &\quad - i\left[-i\left(\frac{\kappa_1}{2}a^\dagger a + \frac{\kappa_2}{2}b^\dagger b + \frac{\gamma_a}{2}\sigma_+\sigma_-\right),\rho\right]_+\\ &= \frac{1}{i\hbar}[\widetilde{H}_1,\rho] + \frac{1}{i\hbar}[\widetilde{H}_2,\rho]_+. \qquad \text{(A2)}\end{aligned}$$

Here $[\ ,\ ]_+$ denotes the anticommutator, and also we have

$$\widetilde{H}_1 = \hbar\Delta(a^\dagger a + b^\dagger b) + \hbar\Delta_a\sigma_+\sigma_- + \hbar J(a^\dagger b + b^\dagger a) + \hbar[(g_a a^\dagger + g_b b^\dagger)\sigma_- + \varepsilon_a a^\dagger + \varepsilon_b b^\dagger e^{-i\delta t} + \text{H.c.}], \tag{A3}$$

$$\widetilde{H}_2 = -i\hbar\frac{\kappa_1}{2}a^\dagger a - i\hbar\frac{\kappa_2}{2}b^\dagger b - i\hbar\frac{\gamma_a}{2}\sigma_+\sigma_-. \tag{A4}$$

Using the above equations, we could describe the system by an effective [76] wave function $|\psi\rangle$. It is obvious that only $\widetilde{H}_1$ is an Hermitian operator, whereas $\widetilde{H}_2$ is not because of the coefficient i. In particular, $\widetilde{H}_1^\dagger = \widetilde{H}_1$ and $\widetilde{H}_2^\dagger = -\widetilde{H}_2$. Using the pure-state approximation of the density operator $\rho \approx |\psi\rangle\langle\psi|$, we get

$$\frac{d|\psi\rangle}{dt}\langle\psi| + |\psi\rangle\frac{d\langle\psi|}{dt} = -i(\widetilde{H}_1|\psi\rangle\langle\psi| - |\psi\rangle\langle\psi|\widetilde{H}_1) - i(\widetilde{H}_2|\psi\rangle\langle\psi| + |\psi\rangle\langle\psi|\widetilde{H}_2), \tag{A5}$$

which can be divided into two subequations

$$\frac{d|\psi\rangle}{dt}\langle\psi| = -i\widetilde{H}_1|\psi\rangle\langle\psi| - i\widetilde{H}_2|\psi\rangle\langle\psi|, \tag{A6}$$

$$|\psi\rangle\frac{d\langle\psi|}{dt} = i|\psi\rangle\langle\psi|\widetilde{H}_1 - i|\psi\rangle\langle\psi|\widetilde{H}_2. \tag{A7}$$

As there is only one solution to the master equation, we consider Eq. (A6) as the equivalent Schrödinger equation of the master equation in Eq. (3). The effective non-Hermitian Hamiltonian of the system is thus given by

$$\begin{aligned}\widetilde{H} &= \widetilde{H}_1 + \widetilde{H}_2 \\ &= \hbar\Delta(a^\dagger a + b^\dagger b) + \hbar\Delta_a\sigma_+\sigma_- + \hbar J(a^\dagger b + b^\dagger a) \\ &\quad + \hbar[(g_a a^\dagger + g_b b^\dagger)\sigma_- + \varepsilon_a a^\dagger + \varepsilon_b b^\dagger e^{-i\delta t} + \text{H.c.}] \\ &\quad - i\hbar\frac{\kappa_1}{2}a^\dagger a - i\hbar\frac{\kappa_2}{2}b^\dagger b - i\hbar\frac{\gamma_a}{2}\sigma_+\sigma_- \\ &= \hbar\Big(\Delta - i\frac{\kappa_1}{2}\Big)a^\dagger a + \hbar\Big(\Delta - i\frac{\kappa_2}{2}\Big)b^\dagger b \\ &\quad + \hbar\Big(\Delta_a - i\frac{\gamma_a}{2}\Big)\sigma_+\sigma_- + \hbar J(a^\dagger b + b^\dagger a) \\ &\quad + \hbar[(g_a a^\dagger + g_b b^\dagger)\sigma_- + \varepsilon_a a^\dagger + \varepsilon_b b^\dagger e^{-i\delta t} + \text{H.c.}].\end{aligned} \tag{A8}$$

In the special case that $\omega_2 = \omega_1$, $\omega_a = \omega$, and $\kappa_1 = \kappa_2$, i.e., $\delta = 0$ and $\Delta = \Delta_a$, Eq. (A8) turns into Eq. (5).

APPENDIX B: DERIVATION OF THE SECOND-ORDER CORRELATION FUNCTION FOR $J = 0$

In this special case, Eq. (18) is reduced to

$$C_{1,0,-} = \frac{B}{\Delta_p A}, \tag{B1}$$

with

$$A = |g_a|^2 + |g_b|^2 - \Delta_d\Delta_p, \tag{B2}$$

$$B = \Delta_d\Delta_p\varepsilon_a + \varepsilon_b g_a g_b^* - \varepsilon_a|g_b|^2. \tag{B3}$$

By setting $J = 0$, we can also solve Eqs. (22)–(26) to obtain

$$C_{2,0,-} = \frac{\sqrt{2}(C + D)}{2\Delta_p^2 AE}, \tag{B4}$$

with

$$C = \Delta_d^2\Delta_p^2\varepsilon_a^2 + \Delta_d\Delta_p^3\varepsilon_a^2 - 2\Delta_d\Delta_p\varepsilon_a^2|g_b|^2 + 2\Delta_d\Delta_p\varepsilon_a\varepsilon_b g_a g_b^* + \Delta_p^2\varepsilon_a^2|g_a|^2, \tag{B5}$$

$$D = -\Delta_p^2\varepsilon_a^2|g_b|^2 + 2\Delta_p^2\varepsilon_a\varepsilon_b g_a g_b^* + \varepsilon_a^2|g_b|^4 - 2\varepsilon_a\varepsilon_b g_a|g_b|^2 g_b^* + \varepsilon_b^2 g_a^2 g_b^{*2}, \tag{B6}$$

$$E = |g_a|^2 + |g_b|^2 - \Delta_p^2 - \Delta_d\Delta_p. \tag{B7}$$

Using Eq. (9), Eq. (B1), and Eq. (B4), the normalized equal-time second-order correlation function is now given as

$$g_{\text{A}}^{(2)}(0) = \frac{|A|^2|C + D|^2}{|B|^4|E|^2}, \tag{B8}$$

which can be further simplified to the expression in Eq. (27).

[1] A. J. Shields, Nat. Photon. **1**, 215 (2007).
[2] S. Buckley, K. Rivoire, and J. Vučković, Rep. Prog. Phys. **75**, 126503 (2012).
[3] A. Scherer, B. C. Sanders, and W. Tittel, Opt. Express **19**, 3004 (2011).
[4] N. Lütkenhaus, Phys. Rev. A **61**, 052304 (2000).
[5] M. A. Nielsen and I. L. Chuang, *Quantum Computation and Quantum Information* (Cambridge University Press, Cambridge, UK, 2000).
[6] T. Jennewein, M. Barbieri, and A. G. White, J. Mod. Opt. **58**, 276 (2011).
[7] A. Kiraz, M. Atatüre, and A. Imamoğlu, Phys. Rev. A **69**, 032305 (2004).
[8] A. I. Lvovsky, B. C. Sanders, and W. Tittel, Nat. Photon. **3**, 706 (2009).
[9] A. E. Kozhekin, K. Molmer, and E. Polzik, Phys. Rev. A **62**, 033809 (2000).
[10] J. I. Cirac, P. Zoller, H. J. Kimble, and H. Mabuchi, Phys. Rev. Lett. **78**, 3221 (1997).
[11] X. Maitre, E. Hagley, G. Nogues, C. Wunderlich, P. Goy, M. Brune, J. M. Raimond, and S. Haroche, Phys. Rev. Lett. **79**, 769 (1997).
[12] V. Giovannetti, S. Lloyd, and L. Maccone, Science **306**, 1330 (2004).
[13] G. S. Agarwal, R. W. Boyd, E. M. Nagasako, and S. J. Bentley, Phys. Rev. Lett. **86**, 1389 (2001).

[14] D. Fattal, K. Inoue, J. Vučković, C. Santori, G. S. Solomon, and Y. Yamamoto, Phys. Rev. Lett. **92**, 037903 (2004).

[15] V. Giovannetti, S. Lloyd, and L. Maccone, Nature (London) **412**, 417 (2001).

[16] I. Bulutas and F. Nori, Science **326**, 108 (2009).

[17] I. M. Georgescu, S. Ashhab, and F. Nori, Rev. Mod. Phys. **86**, 153 (2014).

[18] P. Kwiat, H. Weinfurter, T. Herzog, A. Zeilinger, and M. A. Kasevich, Phys. Rev. Lett. **74**, 4763 (1995).

[19] T. Peyronel, O. Firstenberg, Q.-Y. Liang, S. Hofferberth, A. V Gorshkov, T. Pohl, M. D. Lukin, and V. Vuletić, Nature (London) **488**, 57 (2012).

[20] S. Ferretti, V. Savona, and D. Gerace, New J. Phys. **15**, 025012 (2013).

[21] A. Imamoğlu, H. Schmidt, G. Woods, and M. Deutsch, Phys. Rev. Lett. **79**, 1467 (1997).

[22] P. Grangier, D. F. Walls, and K. M. Gheri, Phys. Rev. Lett. **81**, 2833 (1998).

[23] K. M. Birnbaum, A. Boca, R. Miller, A. D. Boozer, T. E. Northup, and H. J. Kimble, Nature (London) **436**, 87 (2005).

[24] A. Majumdar, M. Bajcsy, A. Rundquist, and J. Vučković, Phys. Rev. Lett. **108**, 183601 (2012).

[25] B. Dayan, A. S. Parkins, T. Aoki, E. P. Ostby, K. J. Vahala, and H. J. Kimble, Science **319**, 1062 (2008).

[26] A. Faraon, I. Fushman, D. Englund, N. Stoltz, P. Petroff, and J. Vučković, Nat. Phys. **4**, 859 (2008).

[27] W. Zhang, Z. Yu, Y. Liu, and Y. Peng, Phys. Rev. A **89**, 043832 (2014).

[28] C. Lang, D. Bozyigit, C. Eichler, L. Steffen, J. M. Fink, A. A. Abdumalikov, M. Baur, S. Filipp, M. P. da Silva, A. Blais, and A. Wallraff, Phys. Rev. Lett. **106**, 243601 (2011).

[29] A. J. Hoffman, S. J. Srinivasan, S. Schmidt, L. Spietz, J. Aumentado, H. E. Türeci, and A. A. Houck, Phys. Rev. Lett. **107**, 053602 (2011).

[30] R. Brouri, A. Beveratos, J. P. Poizat, and P. Grangier, Opt. Lett. **25**, 1294 (2000).

[31] C. Jarlov, É. Wodey, A. Lyasota, M. Calic, P. Gallo, B. Dwir, A. Rudra, and E. Kapon, Phys. Rev. Lett. **117**, 076801 (2016).

[32] W. Xie, Y. Zhu, T. Aubert, Z. Hens, E. Brainis, and D. V. Thourhout, Opt. Express **24**, A114 (2016).

[33] Y. L. Liu, G. Z. Wang, Y.-x. Liu, and F. Nori, Phys. Rev. A **93**, 013856 (2016).

[34] C. Cohen-Tannoudji, B. Diu, and F. Ladoë, *Quantum Mechanics I*, 2nd ed. (Wiley-VCH, New York, 2005).

[35] T. Aoki, B. Dayan, E. Wilcut, W. P. Bowen, A. S. Parkins, T. J. Kippenberg, K. J. Vahala, and H. J. Kimble, Nature (London) **443**, 671 (2006).

[36] K. Srinivasan and O. Painter, Nature (London) **450**, 862 (2007).

[37] D. Gershoni, Nat. Mater. **5**, 255 (2006).

[38] E. Kim, M. D. Baaskea, and F. Vollmer, Lab Chip **17**, 1190 (2017).

[39] B. Min, E. Ostby, V. Sorger, E. Ulin-Avila, L. Yang, X. Zhang, and K. Vahala, Nature (London) **457**, 455 (2009).

[40] K. Srinivasan and O. Painter, Phys. Rev. A **75**, 023814 (2007).

[41] Y. Sun, F. Song, C. Qian, K. Peng, S. Sun, Y. Zhao, Z. Bai, J. Tang, S. Wu, H. Ali, F. Bo, H. Zhong, K. Jin, and X. Xu, ACS Photon. **4**, 369 (2017).

[42] M. P. Bakker, T. Ruytenberg, W. Löffler, A. Barve, L. Coldren, M. P. van Exter, and D. Bouwmeester, Phys. Rev. B **91**, 241305(R) (2015).

[43] J. Kasprzak, S. Reitzenstein, E. A. Muljarov, C. Kistner, C. Schneider, M. Strauss, S. Höfling, A. Forchel, and W. Langbein, Nat. Mater. **9**, 304 (2010).

[44] R. Oulton, Nat. Nanotechnol. **9**, 169 (2014).

[45] A. K. Nowak, S. L. Portalupi, V. Giesz, O. Gazzano, C. D. Savio, P.-F. Braun, K. Karrai, C. Arnold, L. Lanco, I. Sagnes, A. Lemaître, and P. Senellart, Nat. Commun. **5**, 3240 (2014).

[46] S. Hughes and G. S. Agarwal, Phys. Rev. Lett. **118**, 063601 (2017).

[47] C. Schneider, A. Rahimi-Iman, N. Y. Kim, J. Fischer, I. G. Savenko, M. Amthor, M. Lermer, A. Wolf, L. Worschech, V. D. Kulakovskii, I. A. Shelykh, M. Kamp, S. Reitzenstein, A. Forchel, Y. Yamamoto, and S. Höfling, Nature (London) **497**, 348 (2013).

[48] K. Müller, A. Rundquist, K. A. Fischer, T. Sarmiento, K. G. Lagoudakis, Y. A. Kelaita, C. S. Muñoz, E. del Valle, F. P. Laussy, and J. Vučković, Phys. Rev. Lett. **114**, 233601 (2015).

[49] A. Majumdar, P. Kaer, M. Bajcsy, E. D. Kim, K. G. Lagoudakis, A. Rundquist, and J. Vučković, Phys. Rev. Lett. **111**, 027402 (2013).

[50] K. Hennessy, A. Badolato, M. Winger, D. Gerace, M. Atatüre, S. Gulde, S. Fält, E. L. Hu, and A. Imamoğlu, Nature (London) **445**, 896 (2007).

[51] A. Rundquist, M. Bajcsy, A. Majumdar, T. Sarmiento, K. Fischer, K. G. Lagoudakis, S. Buckley, A. Y. Piggott, and J. Vučković, Phys. Rev. A **90**, 023846 (2014).

[52] R. Bose, T. Cai, K. R. Choudhury, G. S. Solomon, and E. Waks, Nat. Photon. **8**, 858 (2014).

[53] H. Oda, A. Yamanaka, N. Ozaki, N. Ikeda, and Y. Sugimoto, AIP Adv. **6**, 065215 (2016).

[54] X. Wang, A. Miranowicz, H. R. Li, and F. Nori, Phys. Rev. A **94**, 053858 (2016).

[55] J. M. Fink, A. Dombi, A. Vukics, A. Wallraff, and P. Domokos, Phys. Rev. X **7**, 011012 (2017).

[56] A. Miranowicz, J. Bajer, M. Paprzycka, Y. X. Liu, A. M. Zagoskin, and F. Nori, Phys. Rev. A **90**, 033831 (2014).

[57] Y.-x. Liu, X.-W. Xu, A. Miranowicz, and F. Nori, Phys. Rev. A **89**, 043818 (2014).

[58] D. C. McKay, R. Naik, P. Reinhold, L. S. Bishop, and D. I. Schuster, Phys. Rev. Lett. **114**, 080501 (2015).

[59] P. J. Leek, M. Baur, J. M. Fink, R. Bianchetti, L. Steffen, S. Filipp, and A. Wallraff, Phys. Rev. Lett. **104**, 100504 (2010).

[60] B. Vlastakis, G. Kirchmair, Z. Leghtas, S. E. Nigg, L. Frunzio, S. M. Girvin, M. Mirrahimi, M. H. Devoret, and R. J. Schoelkopf, Science **342**, 607 (2013).

[61] P. Lähteenmäki, G. S. Paraoanu, J. Hasse, and P. J. Hakonen, Nat. Commun. **7**, 12548 (2016).

[62] Z. H. Peng, S. E. de Graaf, J. S. Tsai, and O. V. Astafiev, Nat. Commun. **7**, 12588 (2015).

[63] M. Pechal, L. Huthmacher, C. Eichler, S. Zeytinoğlu, A. A. Abdumalikov, Jr., S. Berger, A. Wallraff, and S. Filipp, Phys. Rev. X **4**, 041010 (2014).

[64] Z. H. Peng, Y.-x. Liu, J. T. Peltonen, T. Yamamoto, J. S. Tsai, and O. Astafiev, Phys. Rev. Lett. **115**, 223603 (2015).

[65] J. Restrepo, C. Ciuti, and I. Favero, Phys. Rev. Lett. **112**, 013601 (2014).

[66] B.-y. Zhou and G.-x. Li, Phys. Rev. A **94**, 033809 (2016).

[67] J. Restrepo, I. Favero, and C. Ciuti, Phys. Rev. A **95**, 023832 (2017).
[68] K. Usami, A. Naesby, T. Bagci, B. M. Nielsen, J. Liu, S. Stobbe, P. Lodahl, and E. S. Polzik, Nat. Phys. **8**, 168 (2012).
[69] H. Okamoto, T. Watanabe, R. Ohta, K. Onomitsu, H. Gotoh, T. Sogawa, and H. Yamaguchi, Nat. Commun. **6**, 8478 (2015).
[70] I. Mahboob, K. Nishiguchi, H. Okamoto, and H. Yamaguchi, Nat. Phys. **8**, 387 (2012).
[71] J. Bochmann, A. Vainsencher, D. D. Awschalom, and A. N. Cleland, Nat. Phys. **9**, 712 (2013).
[72] Y.-L. Liu, Z.-P. Liu, and J. Zhang, J. Phys. B: At., Mol., Opt. Phys. **48**, 105501 (2015).
[73] L. Fan, K. Y. Fong, M. Poot, and H. X. Tang, Nat. Commun. **6**, 6850 (2015).
[74] Y.-L. Liu, R. Wu, J. Zhang, Ş. K. Özdemir, L. Yang, F. Nori, and Y.-x. Liu, Phys. Rev. A **95**, 013843 (2017).
[75] I. Mahboob, K. Nishiguchi, A. Fujiwara, and H. Yamaguchi, Phys. Rev. Lett. **110**, 127202 (2013).
[76] H J. Carmichael, *Statistical Methods in Quantum Optics 2: Non-Classical Fields* (Springer Science & Business Media, New York, 2009).